The Journal of Experimental Biology 214, 1554-1559

doi:10.1242/jeb.052092

RESEARCH ARTICLE

The shallow turn of a worm

Daeyeon Kim[1], Sungsu Park[2], L. Mahadevan[3] and Jennifer H. Shin[1,4,*]

[1]School of Mechanical, Aerospace and Systems Engineering, Division of Mechanical Engineering, Korea Advanced Institute of Science and Technology, Daejeon 305-701, Republic of Korea, [2]Department of Chemistry and Nano Sciences, Ewha Womans University, Seoul 120-750, Republic of Korea, [3]School of Engineering and Applied Sciences, Department of Organismic and Evolutionary Biology, Harvard University, Cambridge, MA 02138, USA and [4]Department of Bio and Brain Engineering, Korea Advanced Institute of Science and Technology, Daejeon 305-701, Republic of Korea

*Author for correspondence (j_shin@kaist.ac.kr)

Accepted 19 January 2011

SUMMARY

When crawling on a solid surface, the nematode *Caenorhabditis elegans* (*C. elegans*) moves forward by propagating sinusoidal dorso-ventral retrograde contraction waves. A uniform propagating wave leads to motion that undulates about a straight line. When *C. elegans* turns as it forages or navigates its environment, it uses several different strategies of reorientation. These modes include the well-known omega turn, in which the worm makes a sharp angle turn forming an Ω-shape, and the reversal, in which the worm draws itself backwards. In these two modes of reorientation, *C. elegans* strongly disrupts its propagating sinusoidal wave, either in form or in direction, leading to abrupt directional change. However, a third mode of reorientation, the shallow turn, involves a gentler disruption of the locomotory gait. Analyzing the statistics of locomotion suggests that the shallow turn is by far the most frequent reorienting maneuver in navigation in the absence of food. We show that the worm executes a shallow turn by modulating the amplitude and wavelength of its curvature during forward movement, and provide a minimal description of the process using a three-parameter mathematical model. The results of our study augment the understanding of how these parameters are controlled at the neuromotor circuit level.

Supplementary material available online at http://jeb.biologists.org/cgi/content/full/214/9/1554/DC1

Key words: *Caenorhabditis elegans*, turning behavior, off-food navigation.

INTRODUCTION

The worm *Caenorhabditis elegans* generally employs three types of crawling modes on a solid surface: a forward run, a reversal and a turn. In the absence of sensory cues such as chemical or thermal gradients (Pierce-Shimomura et al., 1999), frequent reversals and turns are used to induce random reorientations. However, in the presence of attractants, worms are able to track gradients using a biased random walk (Pierce-Shimomura et al., 1999; Ryu and Samuel, 2002; Zariwala et al., 2003; Luo et al., 2006) by executing persistent forward runs while suppressing directional changes. Similarly, in the absence of food, *C. elegans* switches from a local search behavior of frequent reversals and turns to a long-range roaming behavior characterized by persistent forward movement in attempts to find a new lawn of food (Gray et al., 2005; Samuel and Sengupta, 2005; Wakabayashi et al., 2004). However, navigation in the absence of food, worms also exhibit a large number of small angle turns by forming higher or lower amplitude bends. This 'shallow turn' is distinct from sharp turning modes such as omega and coil turns observed in random reorientation. Whereas omega and coil turns lead to sharp or abrupt changes in direction by shaping the body like an omega or a coil (Gray et al., 2005), the shallow turn leads to a relatively small turning angle change while maintaining a sinusoidal wave. Indeed, in a variety of behaviors in the presence and absence of any external stimuli, the worm uses shallow turns to follow sensory information effectively (Luo et al., 2006; Iino and Yoshida, 2009; Stephens et al., 2010). Although previous work has mentioned the importance of the small angle turning mode, no efforts to analyze or quantify it have been reported thus far (Gray et al., 2005; Luo et al., 2006; Iino and Yoshida, 2009).

Here we experimentally and theoretically characterize the shallow turn mode, quantify its occurrence in behavioral assays and discuss the mechanisms by which it can be controlled.

MATERIALS AND METHODS

Video recording and behavioral assays

Caenorhabditis elegans Maupas 1900 wild-type (strain N2) were cultured at 20°C on nematode growth medium (NGM) plates seeded with *Escherichia coli* OP50, using standard methods (Brenner, 1974). Well-fed young adults were transferred onto 3% (w/v) agar plates and the crawling motions of single worms were recorded for 30 min off-food using a digital video recorder mounted on a stereomicroscope. The worm indents the agar and very conveniently leaves a permanent trace of the worm's path, which makes the analysis of the path easy. We counted the number of each of the three reorientation modes: shallow turns, omega turns and reversals. Coil turns were not considered because they rarely occurred during experiments. We define a shallow turn as one which satisfies three criteria: (1) the worm maintains sinusoidal waves during the turn; (2) the angle (θ) change is in the range of 10–90 deg within a single bend; and (3) the turn is accompanied by straight runs of at least one wavelength (two lateral bends) before and after the turn, which serve as references for a quantitative description of the changes in

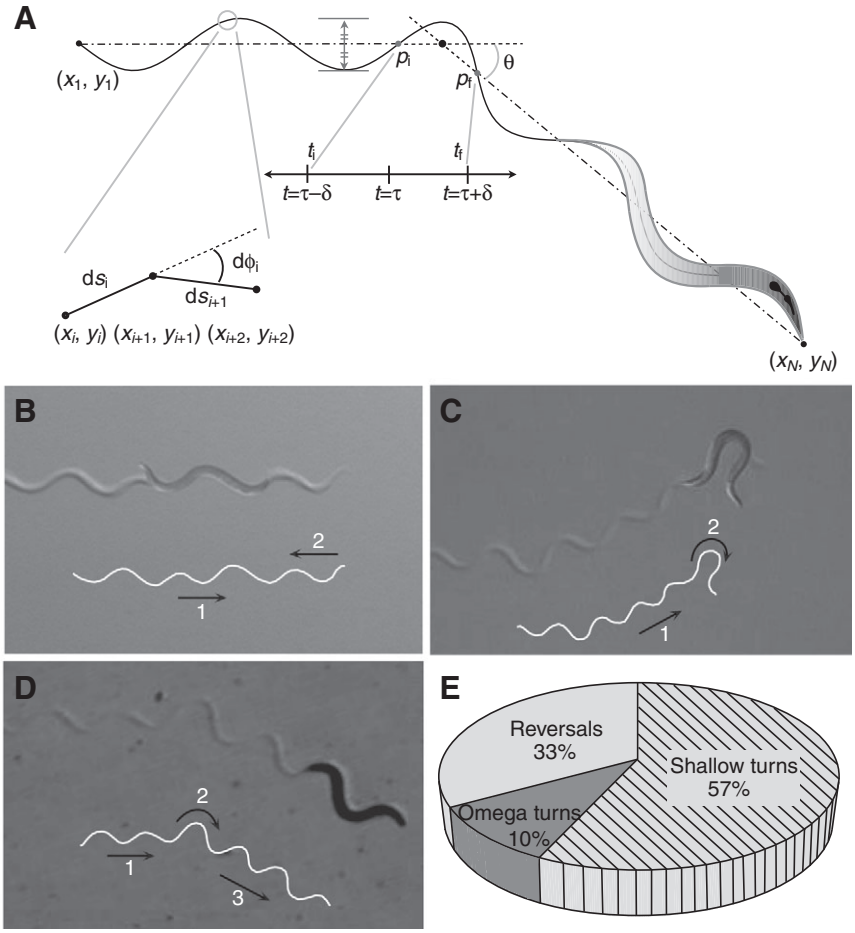

Fig. 1. (A) A schematic diagram of the differential tangent angle ($d\phi_i$) and the differential arc length (ds_i) on a crawling track. The dot-dashed lines show the pre- and post-turning states, and their intersection (dashed lines) characterizes the turning angle θ. Here p_i is the point of turn initiation, p_f is the point of turn termination, t_i is the initiation time of a turn and t_f is the termination time of a turn. (B–D) Typical track patterns of (B) a reversal, (C) an omega turn, and (D) a shallow turn are shown in crawling *C. elegans* (the sequences of motions are indicated by numbers and arrows). (E) Observed frequency of the different reorientation behaviors during the 30 min observation period.

curvature profile during the turn. Thus, a shallow turn can be divided into three phases: pre-turning, turning and post-turning. As illustrated in Fig. 1A, we draw axial lines (represented as a dot-dashed lines) keeping the symmetry in the waves in both the pre-turning and post-turning states. Extensions of these two axial lines (represented as dashed lines) intersect to characterize the turning angle θ. The initiation (p_i) and termination points (p_f) of the turn were defined as the points of intersection between the axial line and the crawling track at the instant of symmetry breakage. The sinusoidal shape is maintained during a shallow turn in forward movement. In contrast, omega turns, with their characteristic Ω-shape, involve the worm bending its whole body to one side and breaking the previous sinusoidal wave in the running state with an obtuse turning angle. Reversals were counted in case of any backward movement of the body, including both short and long reversals (Gray et al., 2005).

Video analysis

The raw track of a worm's shallow turning motion over a few consecutive frames was obtained from recorded video using custom algorithms written in MATLAB (MathWorks, Inc., Natick, MA, USA). Because there are discontinuities in the extracted track at some locations, the raw track was converted to a continuous and smoothly differentiable curve using the smoothing spline method (Reinsch, 1967). The x-coordinate of each point $[x_i, y_i]$ along the curve is equally spaced by 15 μm (i=1:N). We calculated the differential arc length $[ds_i=\sqrt{(x_{i+1}-x_i)+(y_{i+1}-y_i)}]$ and the differential tangent angle ($d\phi_i$) between two consecutive differential arc lengths (ds_i and ds_{i+1}; Fig. 1A). The curvature ($\kappa_i=d\phi_i/ds_i$) was then calculated at each point along the track. The motion of the worm is completely described in terms of this spatio-temporal curvature profile. For a worm that runs forward, the curvature oscillates with a mean of zero. However, when the worm turns, the curvature profile exhibits transient peaks and troughs.

RESULTS

Characterizing the frequency, duration and amplitude of shallow turns in off-food navigation

In the absence of food, the worms utilized three reorientation modes between runs (reversals, omega turns and shallow turns) to freely navigate the environment, and a typical track pattern is shown in Fig. 1B–D. A pie chart of the different reorientation behaviors (Fig. 1E) indicates that the shallow turn is the most dominant mode of turning during the observation period.

In order to quantify the individual reorientation maneuvers, we first analyzed the amplitude of the turn characterized by the turning angle (θ), where a reversal is assigned a turning angle of zero because it does not involve a real turning motion. The results show that turning angles had a normal distribution centered at zero, indicating that reorientation events with large turn angles seldom occurred (Fig. 2A). Instead, most reorientation events had low turn angles in the range of 0 to 60 deg, which correspond to shallow turns. These results suggest that the shallow turn is the most predominant turning strategy among reorientation modes in the absence of food.

To examine shallow turns at a more detailed level, we next analyzed the statistics of the normalized duration of a turn in terms of the dimensionless quantity $2\delta v/L$, the travelling distance during

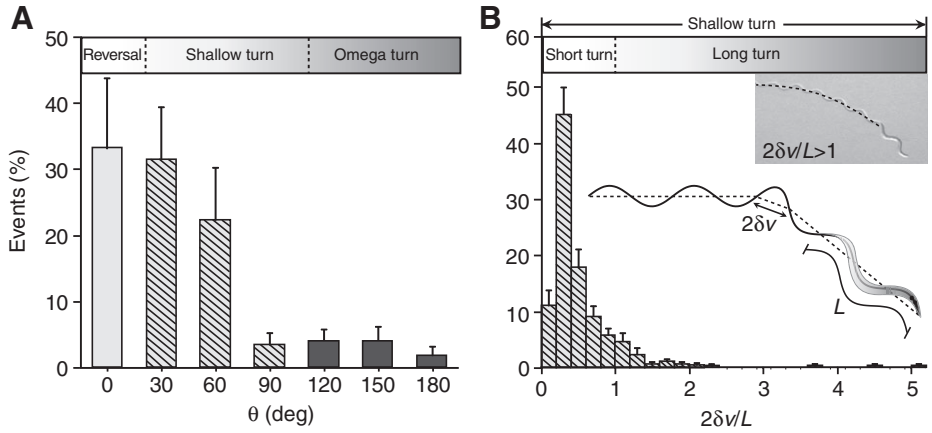

Fig. 2. (A) Percentages of three reorientation modes are plotted as a function of turning angles (means ± s.d., n=7 worms, N=1166 events). Large turn angles show rare occurrence while small angle turns in the range of 0–60 deg are predominant. (B) Shallow turns can be categorized into short and long turns depending on the duration over which the turn is complete. $2\delta v/L$ is the traveled distance normalized by body length where 2δ is the duration of a turn, and v/L is the forward speed normalized by the body length of worm (means ± s.e.m., n=5 worms, N=426 events). The inset shows a typical trajectory of long turn with $2\delta v/L>1$ where a worm makes long turns by changing the angle of direction slowly.

the turn normalized by the body length, where 2δ is the duration of a turn in the dimension of time, v is the forward speed and L is the body length of the worm. We define a short shallow turn as one that completes the curvature change within one body length. In this case, the travelling distance during the turn normalized by body length is $2\delta v/L\leq 1$. A long shallow turn is one that is carried out over more than one body length, $2\delta v/L>1$. The distribution of shallow turns as a function of their duration indicates that, for most shallow turns, $2\delta v/L\leq 1$ (Fig. 2B); thus they typically correspond to situations such as that shown in Fig. 1D, where a turn is completed within a body length. There were, however, a few cases when the normalized duration of the shallow turns was large, i.e. $2\delta v/L>1$, when the worm made long turns by slowly changing the angle of direction (see Fig. 2B inset).

Next, we characterized the variation in the curvature and local orientation during a shallow turn, because the curvature of the centerline of the worm is a natural shape invariant. In Fig. 3A,B we show that worms exhibit two fundamental modes of shallow turns, S1 and S2; these turns have a transient maximum or minimum in the curvature (marked with asterisks) with $2\delta v/L\leq 0.2$, respectively (supplementary material Movies 1, 2). The S1 and S2 turns are minimal ways of modulating the curvature within a single bend, showing a single transient peak or dip in the curvature profile. In each case, the turn consists of two parts separated by a transient peak or dip in the curvature. Two experimentally measurable quantities that characterize these turns are the amplitude κ_{max} and wavelength Λ of the curvature profile. In Fig. 3A–C we show that the S1 turn is characterized by a simultaneous increase in both κ_{max} and Λ whereas the S2 turn is characterized by a decrease in both of these quantities transiently during the turn.

Although this simple characterization suffices as a beginning, we now turn to a mathematical description of the shallow turning process itself.

Minimal mathematical description of a shallow turn

We start by emphasizing that the goal of this mathematical exercise is not to provide a mechanistic explanation of turning in terms of the neuromuscular control strategies, but to extract a minimal set of parameters that characterize a turn and thus more accurately specify the mechanism for this unsteady motion.

A shallow turn can be characterized by its turning angle and duration of a turn, as well as the phase of the initiation of a turning maneuver relative to the naturally periodic undulations of the worm. A mathematical representation of turning using these three primitive parameters requires the choice of an initial direction associated with the orientation of the worm (chosen to be along the x-axis) as well as the undulation speed v, frequency ω and amplitude A. Because the head of the worm leads the body everywhere, it is sufficient to describe the position of the head $[x(t), y(t)]$ and its velocity, which is given by:

$$\dot{x} = v + [v\cos\theta - v - A\omega\cos(\omega t)\sin\theta] \times \frac{1}{2}\left\{1 + \tanh\left[\frac{1}{\delta}(t-\tau)\right]\right\}, \quad (1)$$

$$\dot{y} = A\omega\cos(\omega t) + [(\cos\theta - 1)A\omega\cos(\omega t) + v\sin\theta] \times \frac{1}{2}\left\{1 + \tanh\left[\frac{1}{\delta}(t-\tau)\right]\right\}, \quad (2)$$

where τ/δ is the relative phase of a turn and 2δ is the duration of a shallow turn, because we set the initiation time (t_i) and termination time (t_f) for a turn as $t_i=\tau-\delta$ and $t_f=\tau+\delta$, respectively.

Thus we see that the velocity before the beginning of a turn is:

$$\dot{x} = v,\ \dot{y} = A\omega\cos(\omega t);\ t < \tau - \delta, \quad (3)$$

and after the turn:

$$\dot{x} = v\cos\theta - A\omega\cos(\omega t)\sin\theta,\ \dot{y} = v\sin\theta + A\omega\cos(\omega t)\cos\theta;\ t > \tau + \delta, \quad (4)$$

while the curvature of the path is given by:

$$\kappa(t) = \frac{\dot{x}\ddot{y} - \dot{y}\ddot{x}}{(\dot{x}^2 + \dot{y}^2)^{3/2}}. \quad (5)$$

For steady, effectively rectilinear motion, $x=vt$ and $y=A\sin(\omega t)$, so that the curvature is periodic with a maximum of $A\omega^2/v^2$. Then the normalized contour length of the worm in one period Λ/L is given by:

$$\Lambda/L = \frac{1}{L}\int ds = \frac{1}{L}\int_{x=0}^{\lambda}\sqrt{1+(dy/dx)^2}\,dx = \frac{1}{L}\int_0^T \sqrt{1+[(A\omega/v)\cos(\omega t)]^2}\,v\,dt = v/(L\omega)\times\sqrt{1+(A\omega/v)^2}\times 4E(q), \quad (6)$$

where λ is the wavelength of undulations ($\lambda=2\pi v/\omega$), $E(q)$ is the complete elliptic integral of the second kind and $q=(A\omega/v)^2/[1+(A\omega/v)^2]$. During a turn, the worm changes both the amplitude κ_{max} and the wavelength Λ of its curvature; an increase or decrease in these two parameters results in two different types of shallow turns, S1 and S2. Interpreting the consequence of these

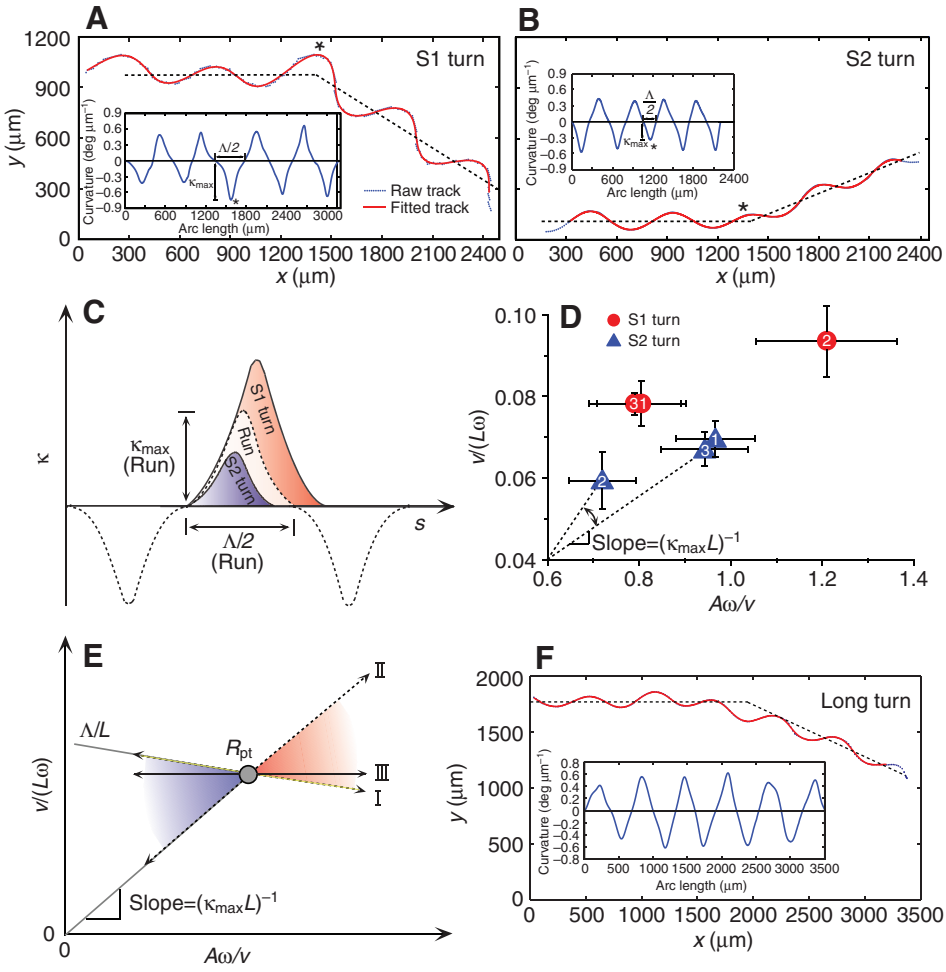

Fig. 3. (A,B) Trajectories and corresponding curvature profiles of the experimentally observed S1 (A) and S2 (B) shallow turns. Turning events with a transient maximum (or minimum) in curvature are marked with asterisks. The turning angles (θ) of the S1 and S2 turns are –30.45 and 19.59 deg, respectively. During the S1 turn, both κ_{max} and $\Lambda/2$ are increased whereas both quantities are reduced during the S2 turn. This trend is summarized in a schematic diagram of curvature profiles in C. (D) In the phase space of $A\omega/v$ and $v/(L\omega)$, real worms exhibit a moderate increase (decrease) in $v/(L\omega)$ and a significant increase (decrease) in $A\omega/v$ for S1 (S2) turns by modulating A, v and ω (means ± s.d., N=10 events for S1 turns and 8 events for S2 turns). Among the 426 shallow turns in Fig. 2B, a total of 18 S1 and S2 turns with θ of 35–40 deg are selected for statistical analysis in the phase space of $A\omega/v$ and $v/(L\omega)$. 1, 2 and 3 correspond to the pre-turning, turning and post-turning states, respectively. (E) Schematic diagrams of pathways for S1 and S2 shallow turns are illustrated in the phase space of $A\omega/v$, $v/(L\omega)$. R_{pt} represents a pre-turning state and a worm can make a decision to make an S1 or S2 shallow turn by modulating the curvature profile. Lines marked as I and II represent the extreme pathways that regulate only κ_{max} or Λ, keeping the other quantity constant, respectively. The red region to the right of R_{pt} represents the S1 turn (where both κ_{max} and Λ increase) and the blue region to the left of R_{pt} represents the S2 turn (where both κ_{max} and Λ decrease). The pathway III represents the cases of the simulated S1 and S2 turns where the speed and frequency of undulation are constant while only the curvature amplitude in undulation changes. (F) A trajectory and corresponding curvature profile of an experimentally observed long shallow turn with $2\delta v/L>1$. The modulation of curvature is accomplished in the long range of arc length during the turn, resulting in no apparent peak or dip in the curvature profile.

changes in curvature profiles in the phase space of $A\omega/v$ and $v/(L\omega)$, we see that real worms exhibit a moderate increase (decrease) in $v/(L\omega)$ and a significant increase (decrease) in $A\omega/v$ for S1 (S2) turns by modulating A, v and ω. We confirm these characteristics of S1 and S2 turns through a statistical analysis of the curvature as shown in Fig. 3D.

We use the phase space of $A\omega/v$ and $v/(L\omega)$ to illustrate a few of the (infinite) possibilities of executing S1 and S2 turns starting from the pre-turning state (denoted as R_{pt} where A, v, ω and L are constant; Fig. 3E). Two extreme ways to produce S1 and S2 turns are to: (1) modulate only κ_{max} while keeping Λ constant along the straight line represented by 'I' or (2) change only Λ while keeping κ_{max} constant along the straight line 'II'. Moving rightwards along 'I' from R_{pt} leads to an increase in κ_{max} during the S1 turn whereas traveling leftwards along 'I' leads to a decrease in κ_{max} during the S2 turn. Similarly, moving rightwards along 'II' from R_{pt} represents an increase in Λ during the S1 turn whereas traveling leftwards along 'II' leads to a decrease in Λ during the S2 turn. As evidenced in Fig. 3A–C, *C. elegans* modulate both κ_{max} and Λ during turns, with a positive correlation between them; thus the red region represents the S1 turn with higher κ_{max} and Λ relative to R_{pt} whereas the blue region represents the S2 turns with lower κ_{max} and Λ relative to R_{pt}. So far, we have assumed that turning is accommodated by modulating the curvature while the speed v and the frequency of undulation ω are kept constant (v=150 µm s^{-1} and ω=1.8 rad s^{-1}), as represented by 'III' in Fig. 3E.

Then, integrating Eqns 1 and 2 with respect to time yields the entire trajectory of the head (and thus the body that follows). In

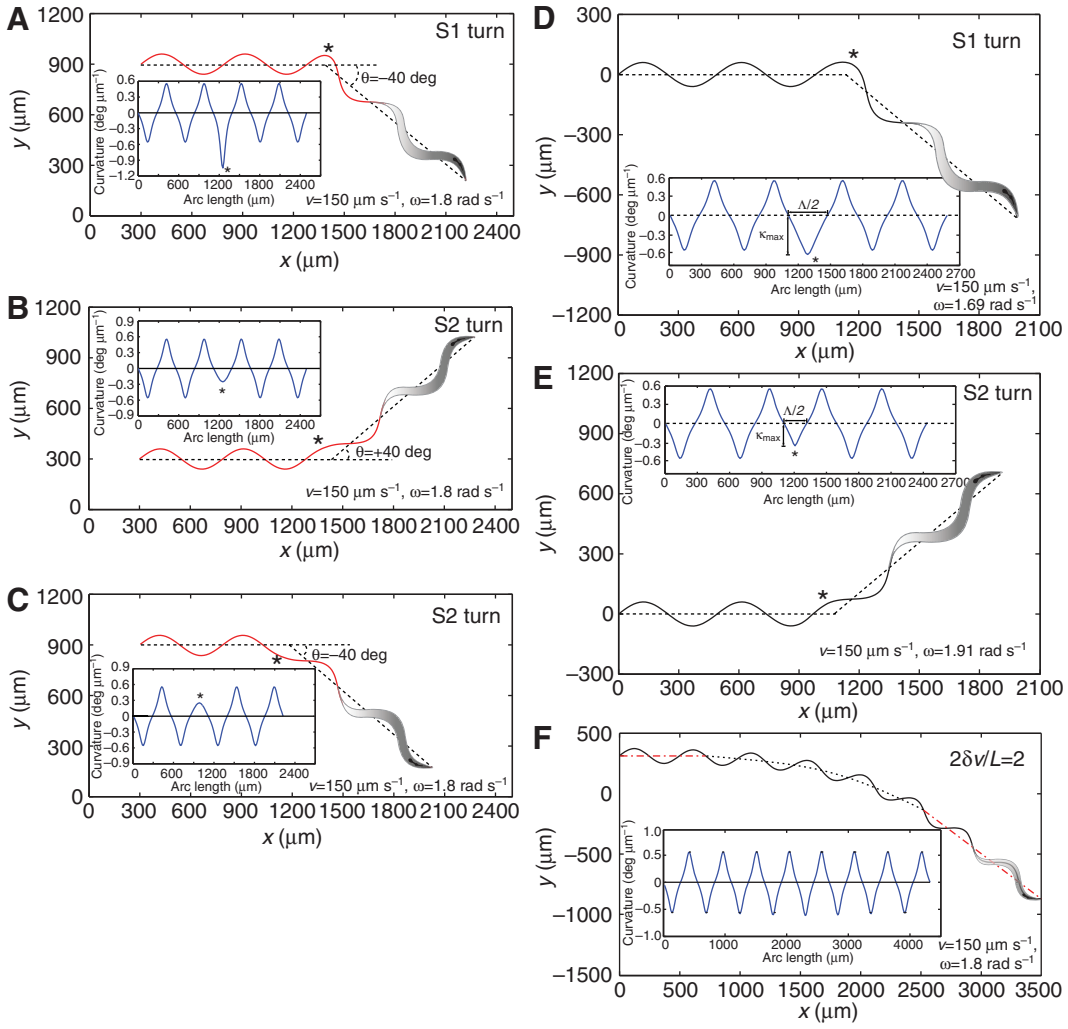

Fig. 4. (A–C) Trajectories and their curvature profiles (insets) of the simulated worms. Turning events with a transient maximum (or minimum) in curvature are marked with asterisks. As in the experimentally observed worms, simulated worms exhibit turns consisting of two parts separated by a transient peak or dip in the curvature. Given the constant values for the speed and frequency of undulation (v=150 μm s^{-1}, ω=1.8 rad s^{-1}), if the duration and phase of a turn are fixed as $2\delta v/L$=0.1 and τ/δ=22, respectively, opposite signs of turning angles (+40 or –40 deg) lead to (A) S1 and (B) S2 turns, respectively. However, when the duration and turning angle of a turn are fixed as $2\delta v/L$=0.1 and θ=–40 deg, two different phase values of τ/δ=22 and 17.6 give rise to (A) S1 and (C) S2 turns, respectively. (D) The simulated S1 and S2 turns with additional modulation of ω to 1.69 and 1.91 rad s^{-1} during the turn, respectively. By relaxing the constraint on frequency, both κ_{max} and Λ show a consistent increase (S1) and decrease (S2) in the curvature profiles, better representing the real worm's shallow turns. (F) Trajectory and corresponding curvature profile of the simulated worm with $2\delta v/L$=2, representing the long turns shown in Fig. 2B (inset) and Fig. 3F. Other simulating parameters are kept identical to those in A. Dot-dashed lines, mean trajectory of the worm in its pre- and post-turning states; dotted line, path traversed during the turn.

general, there are two ways to get S1 and S2 turns: by either keeping the relative phase of the initiation of a shallow turn τ/δ constant while changing the sign of the turning angle θ or *vice versa*. The normalized duration of a shallow turn $2\delta v/L$ determines if the turn is short or long (see Fig. 2B) but does not influence the type of turn, as we discuss later. For short turns, the traveling distance normalized by body length ($2\delta v/L$) is <1; for example, as v/L=0.15, we fix the normalized duration of a turn $2\delta v/L$=0.1. Then, given the phase of a turn τ/δ=22, changing the sign of the turning angle from –40 to +40 deg causes an S1 turn to become an S2 turn and *vice versa*, as shown in Fig. 4A,B. We see that the curvature profiles of the simulated tracks have the same transient peaks as real worms. However, if the normalized duration of a turn $2\delta v/L$=0.1 and turning angle θ=–40 deg are fixed, different phase values of the phase lead to S1 and S2 turns, as shown in Fig. 4A,C (for τ/δ=22 and 17.6). In this case, S1 and S2 turns lead to net turning in the same direction but with different curvature amplitudes.

By relaxing our constraint on the constancy of the undulatory frequency, and changing ω from 1.8 rad s^{-1} (pre-turning) to 1.69 or 1.91 rad s^{-1}, simulated trajectories for the S1 and S2 turns (Fig. 4D,E) allow us to see that the curvature modulation measures κ_{max} and Λ now mimic the values for real worms more closely. The change in the amplitude of undulations we used in Fig. 4A–C is the minimal way to modulate the experimentally measurable variables κ_{max} and Λ, leading to S1 and S2 turns but relaxation of other two variables, namely speed and frequency of undulation, which potentially improves the simulation to better represent the turning behavior of real worms. By increasing the normalized duration of the turn, a real worm can make shallow turns extend over a longer time (see Fig. 2B inset and Fig. 3F), corresponding

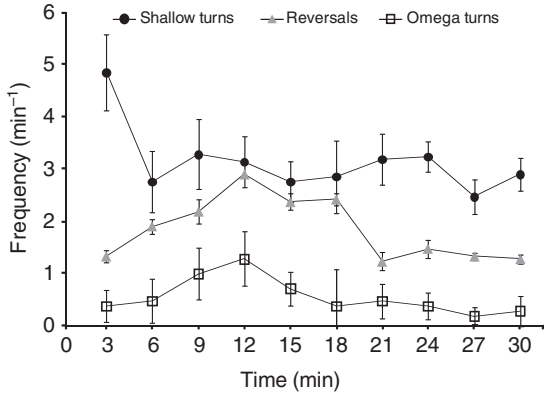

Fig. 5. Frequency distributions of shallow turns, reversals and omega turns plotted as a function of time for the 30 min of observation binned into 3 min intervals. During the entire period, shallow turns had the consistently highest occurrence frequency compared with the other two modes (means ± s.e.m., n=7 worms).

to the case when $2\delta v/L>1$, with a continuous slow modulation of curvature over the duration of the entire turn with no apparent peak or dip in the curvature profile. In Fig. 4F, we show a simulation of a long shallow turn using $2\delta v/L=2$ to capture this type of scenario. Finally, the worm can use sequences of the curvature modulations (S1 and S2 shallow turns) in different permutations that lead to large turning angles and even go around in circles, as shown in supplementary material Fig. S1.

DISCUSSION

Animals respond to their environment through movement. Thus, understanding the origins of animal behavior requires a deconstruction of the basic locomotory gaits and transitions between them in response to external stimuli. Turning is a fundamental way by which *C. elegans* reorients itself in response to the presence or absence of external stimuli. Our study on the characteristic reorientation behavior of *C. elegans* during navigation in the absence of food as it crawls on a substrate shows that the hitherto poorly studied shallow turn is the most frequent reorientation mode.

It may thus be useful to cast our study in a behavioral context. Why do worms execute shallow turns during navigation in the absence of food? To understand this, we counted the number of different reorientation modes (reversals, omega turns and shallow turns) during 30 min of observation binned into 3 min intervals (Fig. 5). During the entire period, shallow turns consistently had the highest occurrence frequency compared with the other two modes. This time-dependent behavior of worms can lead to the interpretation of searching strategies of the worm in navigation in the absence of food. Similarly to the case of chemotaxis, in the absence of food, *C. elegans* switches from a local search behavior of frequent reversals and turns, marked by transient peaks, to a long-range roaming behavior characterized by persistent forward movement and small-angle shallow turns in attempts to find a new lawn of food more effectively. We also note that the occurrence frequency of the shallow turns was the highest during the first 3 min bin, which may have been caused by the mechanical stimulus associated with placing the worm on a new plate.

To characterize shallow turns, we used a simple mathematical model with parameters that describe the amplitude, normalized duration and phase of a turn, and demonstrated that these parameters are sufficient to quantitatively describe turns in a variety of situations involving real worms. Our study raises the obvious and interesting question of how the muscle contractions are coordinated during a turn. One plausible scenario is that contractions could be directly regulated by a motor neuron and an interneuron that gives feedback to the motor neuron. Recently, Gray et al. reported that ablating SMB neurons led to a dramatic increase in the amplitude of sinusoidal movement (Gray et al., 2005). In addition, the removal of one side of SMB and SMD neurons caused worms to make a circle during forward motion. (SMB and SMD are motor neurons that innervate muscles in the head and neck.) Interestingly, DVA interneuron, a pre-synaptic neuron of SMB, is known as a stretch receptor that could provide feedback information on the extent of muscle contraction (Li et al., 2006). When SMB neurons receive a turning signal from interneurons, as known in the case of omega turns (Samuel and Sengupta, 2005), they could regulate the strength and period of stimulation of the curvature in the worm. Clearly, more research is needed to determine what lies 'beneath the hood' of this engine, but the ease of executing a shallow turn by weak asymmetric modulations of the curvature periodicity, amplitude and phase suggest that this is a natural place to start.

ACKNOWLEDGEMENTS

We thank Changmok Choi, Hyejin Hwang, Myung Kyu Choi and Junho Lee for insightful discussion on this work. This work was supported by the National Research Foundation (NRF) grant 2010-0016886 and KAIST KI for Design of Complex Systems.

REFERENCES

Brenner, S. (1974). The genetics of *Caenorhabditis elegans*. *Genetics* **77**, 71-94.
Gray, J. M., Hill, J. J. and Bargmann, C. I. (2005). A circuit for navigation in *Caenorhabditis elegans*. *Proc. Natl. Acad. Sci. USA* **102**, 3184-3191.
Iino, Y. and Yoshida, K. (2009). Parallel use of two behavioural mechanisms for chemotaxis in *Caenorhabditis elegans*. *J. Neurosci.* **29**, 5370-5380.
Li, W., Feng, Z., Sternberg, P. W. and Xu, X. Z. S. (2006). *A C. elegans* stretch receptor neuron revealed by a mechanosensitive TRP channel homologue. *Nature* **440**, 684-687.
Luo, L., Clark, D. A., Biron, D., Mahadevan, L. and Samuel, A. D. T. (2006). Sensorimotor control during isothermal tracking in *Caenorhabditis elegans*. *J. Exp. Biol.* **209**, 4652-4662.
Pierce-Shimomura, J. T., Morse, T. M. and Lockery, S. R. (1999). The fundamental role of pirouettes in *Caenorhabditis elegans* chemotaxis. *J. Neurosci.* **19**, 9557-9569.
Reinsch, C. (1967). Smoothing by spline functions. *Numer. Math.* **10**, 177-183.
Ryu, W. S. and Samuel, A. D. T. (2002). Thermotaxis in *Caenorhabditis elegans* analyzed by measuring responses to defined thermal stimuli. *J. Neurosci.* **22**, 5727-5733.
Samuel, A. D. T. and Sengupta, P. (2005). Sensorimotor integration: locating locomotion in neural circuits. *Curr. Biol.* **15**, R341-R343.
Stephens, G. J., Johnson-Kerner, B., Bialek, W. and Ryu, W. S. (2010). From modes to movement in the behavior of *Caenorhabditis elegans*. *PLoS ONE* **5**, e13914.
Wakabayashi, T., Kitagawa, I. and Shingai, R. (2004). Neurons regulating the duration of forward locomotion in *Caenorhabditis elegans*. *Neurosci. Res.* **50**, 103-111.
Zariwala, H. A., Miller, A. C., Faumont, S. and Lockery, S. R. (2003). Step response analysis of thermotaxis in *Caenorhabditis elegans*. *J. Neurosci.* **23**, 4369-4377.